https://doi.org/10.5194/bg-2019-279
Preprint. Discussion started: 18 September 2019

Biogeosciences Discussions
Open Access
EGU

Carbon dioxide and methane fluxes from different surface types in a created urban wetland

Xuefei Li[1], Outi Wahlroos[2], Sami Haapanala[3], Jukka Pumpanen[4], Harri Vasander[5], Anne Ojala[1, 5, 6] Timo Vesala[1, 5] and Ivan Mammarella[1]

[1]Institute for Atmospheric and Earth System Research (INAR)/Physics, Faculty of Science, University of Helsinki, P.O. Box 68, 00014 University of Helsinki, Finland

[2]University of Turku, Turku, Finland

[3]Suvilumi, Ohrahuhdantie 2 B, 00680 Helsinki, Finland

[4]Department of Environmental and Biological Sciences, University of Eastern Finland, P.O. Box 1627, 70211 Kuopio, Finland

[5]Institute for Atmospheric and Earth System Research (INAR)/Forest Sciences, Faculty of Agriculture and Forestry, University of Helsinki, P.O. Box 27, 00014 University of Helsinki, Finland

[6]Ecosystems and Environment Research Programme, Faculty of Biological and Environmental Sciences, University of Helsinki, P.O. Box 65, 00014 University of Helsinki, Finland

Correspondence to: Xuefei Li (xuefei.z.li@helsinki.fi)

https://doi.org/10.5194/bg-2019-279
Preprint. Discussion started: 18 September 2019

Biogeosciences Discussions Open Access EGU

Abstract. Many wetlands have been drained due to urbanization, agriculture, forestry or other purposes, which has resulted in losing their ecosystem services. To protect receiving waters and to achieve services such as flood control and stormwater quality mitigation, new wetlands are created in urbanized areas. However, our knowledge of greenhouse gas exchange in newly created wetlands in urban areas is currently limited. In this paper we present measurements carried out at a created urban wetland in boreal climate.

We conducted measurements of ecosystem CO_2 flux (NEE) and CH_4 flux (F_{CH4}) at the constructed stormwater wetland Gateway in Nummela, Vihti, Southern Finland using eddy covariance (EC) technique. The measurements were commenced the fourth year after construction and lasted for one full year and two subsequent growing seasons. Besides ecosystem scale fluxes measured by EC tower, the diffusive CO_2 and CH_4 fluxes from the open-water area (F_w_CO_2 and F_w_CH_4, respectively) were modelled based on measurements of CO_2 and CH_4 concentration in the water. Fluxes from vegetated area were estimated by applying a simple mixing model using above-mentioned fluxes and footprint-weighted fractional area. The half-hourly footprint-weighted contribution of diffusive fluxes from open water ranged from 0 to 25.5 % in year 2013.

The annual NEE of the studied wetland was 8.0 g C-CO_2 m^{-2} yr^{-1} with the 95 % confidence interval between -18.9 and 34.9 g C-CO_2 m^{-2} yr^{-1} and F_{CH4} was 3.9 g C-CH_4 m^{-2} yr^{-1} with the 95 % confidence interval between 3.75 and 4.07 g C-CH_4 m^{-2} yr^{-1}. The ecosystem sequestered CO_2 during summer months (June-August), while the rest of the year it was a CO_2 source. CH_4 displayed strong seasonal dynamics, higher in summer and lower in winter, with a sporadic emission episode in the end of May 2013. Both CH_4 and CO_2 fluxes, especially those obtained from vegetated area, exhibited strong diurnal cycle during summer with synchronized peaks around noon. The annual F_w_CO_2 was 297.5 g C-CO_2 m^{-2} yr^{-1} and F_w_CH_4 was 1.73 g C-CH_4 m^{-2} yr^{-1}. The peak diffusive CH_4 flux was 137.6 nmol C-CH_4 m^{-2} s^{-1}, which was synchronized with the F_{CH4}.

Overall, during the monitored time period, the established stormwater wetland had a climate warming effect with 0.263 kg CO_2-eq m^{-2} yr^{-1} of which 89 % was contributed by CH_4. The radiative forcing of the open-water exceeded the vegetation area (1.194 kg CO_2-eq m^{-2} yr^{-1} and 0.111 kg CO_2-eq m^{-2} yr^{-1}, respectively), which implies that, when considering solely the climate impact of a created wetland over a 100-year horizon, it would be more beneficial to design and establish wetlands with large patches of emergent vegetation, and to limit the areas of open-water to the minimum necessitated by other desired ecosystem services.

1 Introduction

Wetlands provide many beneficial ecosystem services such as flood control and water quality mitigation, natural habitat for flora and fauna and recreational opportunities (Mitsch and Gosselink, 2015). Many wetlands have been drained globally for agriculture, forestry and other purposes including urbanization at the cost of losing wetland ecosystem services (Vasander et al., 2003). Migration from rural area to cities will increase in even greater number in the near future, and UN 2016 report has predicted that 75 % of the world population will be living in cities by 2030. There is an urgent need for more sustainable urbanism and one effective measure is to create functional and connected wetland networks in cities (Lucas et al., 2015;Mungasavalli and Viraraghavan, 2006).

Wetlands can take up carbon dioxide (CO_2) through emergent and submerged vegetation but they are also important sources of methane (CH_4), a greenhouse gas more potent than CO_2 when considered over a 100-year horizon (Stocker et al., 2014). The exchange of greenhouse gases (GHG) such as CO_2 and CH_4 between atmosphere and ecosystem have

https://doi.org/10.5194/bg-2019-279
Preprint. Discussion started: 18 September 2019

direct influence on the atmospheric concentration of these gases, thus besides the ecosystem services that wetland provide, the GHG budget of constructed wetlands should be accounted for according to international agreements such as the Kyoto protocol.

Reports on boreal wetlands, such as peatlands, have shown that large carbon storage remains in the soil due to anaerobic conditions limiting microbial decomposition, and thus offering a global cooling effect (Frolking et al., 2006). However, in newly constructed urban wetlands on mineral soil the gas exchange may be very different from natural wetlands: 1) the cooling effect of a wetland may be reduced or it becomes a source of carbon due to the early successional stage of the wetland, 2) wetlands in close proximity to urban centers receive significant amount of nutrients and dissolved organic carbon from runoff and 3) urban wetlands exhibit high spatial heterogeneity and hydrology where different processes of the production and transportation of GHG are involved. At the areas with emergent vegetation, CO_2 is absorbed by photosynthetic activity during daytime and growing season and is released through respirational processes. At open-water surfaces, the net production of CO_2 is a result of photosynthesis by algae, cyanobacteria as well as submerged aquatic plants, respiration of organic carbon and oxidation of CH_4 produced in the water. When the CO_2 concentration in the water exceeds atmospheric equilibrium, the surface becomes a source of CO_2. CH_4 can be produced through anaerobic metabolism in wetland soil and can be transported to the atmosphere by plant-mediated pathway through aerenchyma, sediment ebullition and diffusive fluxes at water-atmosphere interface. In open water, the transport is dominated by diffusion whereas in vegetated area the plant-mediated transport is most prominent.

Urban wetlands have received extensive attention globally and their societal and economical importance have been evaluated (Salminen et al., 2013), whereas their climate impact is still largely overlooked except for only a few studies (e.g. Morin et al., 2014a;Morin et al., 2014b). The only review of GHG emission in constructed wetlands for wastewater treatment reported that the average CO_2 emission was 92.3 mg CO_2-C m^{-2} h^{-1} and that the CH_4 emission ranged from 1.6 to 27 mg CH_4-C m^{-2} h^{-1} from free water surface (Mander et al., 2014). All of the studies were based on static chamber measurements during a short period so that the annual carbon balance of the ecosystem could not be assessed. In contrast to static chamber measurements, eddy covariance (EC) method provides continuous measurements of GHG exchange at ecosystem scale, presenting the net result of fluxes as exchange in different source area contributing simultaneously within the footprint extent (Baldocchi, 2003). It is worth noticing that one of the assumptions of the EC method is surface homogeneity, yet in many study sites the situation are far from ideal. The change of source area due to changes in wind provides difficulties in estimating GHG emissions in spatially heterogeneous sites especially in short-term flux measurements (Baldocchi et al., 2012). Therefore, for heterogeneous sites such as urban wetlands, accurate footprint modelling and surface area map at high spatial resolution are important in identifying the source area, and a land-surface specific analysis is vital to reveal the diel pattern, sink/source strength of the wetland.

The objective of this study is to investigate how CO_2 and CH_4 surface-atmosphere exchange vary with seasonality and spatial heterogeneity and what the annual radiative forcing of these gases are in a constructed urban wetland near town Nummela, Municipality of Vihti, Southern Finland. The studied Gateway wetland was designed and implemented to serve the purposes of stormwater quality treatment, creating an urban park, as well as supporting biodiversity. Besides taking advantage of ecosystem-scale EC measurements, we also parse the variability of gas exchange induced by surface heterogeneity (open water and vegetated area) using diffusional flux modeling and footprint modelling overlapped on a high-resolution surface map. To illustrate how the urban wetland functions as a source or a sink of GHG equivalents, we

https://doi.org/10.5194/bg-2019-279
Preprint. Discussion started: 18 September 2019

calculate separately the sustained global warming potential (SGWP) of CO_2 and CH_4 over a hundred-year horizon in each surface type.

2 Materials and Methods

2.1 Site description

Our study site is a created stormwater wetland Gateway, located by an eutrophicated Lake Enäjärvi in the District of Nummela, Municipality of Vihti, Southern Finland (60.3272°N, 24.3369°E). Southern Finland experiences a climate with a 30-year mean air temperature of 4.6 °C and an annual precipitation rate of 627 mm in the period of year 1981-2010 (Pirinen et al., 2012).

The wetland was constructed in 2010 at the mouth of a 550 hectare largely urbanized (35 % impervious) watershed of Stream Kilsoi. It was excavated over six weeks in early winter 2010 on an abandoned agricultural field growing meadow vegetation. All of the old drainage ditches were blocked as amphibian habitats, which also ensured only one inlet route receiving water from Stream Kilsoi and one outlet route discharging water to the nearby Lake Enäjärvi. Lake Enäjärvi is a eutrophicated lake. The internal phosphorus load from human activities and the run-off from its catchments have resulted in regular cyanobacterial blooms and fish kills in the lake.

The wetland park has a total area of 7 hectares within which - during mean water flow conditions - a 0.5 hectare inundated wetland is located. This stormwater treatment wetland consists of an inlet stilling pond, a meandering shallow water area with three habitat islands, and an outlet pond. The average water depth in the ponds is 1.5 m; within emergent vegetation patches water depth ranges between 0.3 and 0.5 m. There are also submerged macrophytes in the open water as the water is shallow, thus in the paper we refer the “vegetated area” to the area with emergent vegetation and “open water” to the area covered by water in the absence of emergent macrophytes. The outlet bottom dam sets low water level (WL) to 50.04 m above the Baltic Sea level (N60+ coordinate system). Herbaceous vegetation has been allowed to fully self-establish after the construction of the wetland. Annual monitoring of vegetation carried out in summers 2010, 2011 and 2012 indicated rapid self-establishment of vegetation which was rich in taxa and dominated by native species (Wahlroos et al., 2015). At frequently-inundated area (elevation levels of 50-50.35 m), vegetation was arranged in dense patches with different dominating wetland plant species: *Typha latifolia* L., *Iris pseudacorus* L., *Carex* spp. or *Juncus effuses* L. At the major less-frequently inundated area (elevation levels of 50.35-50.45m), the wet meadow species *Filipendula ulmaria* L. (Maxim.), *Lysimachia vulgaris* L., and *Lythrum salicaria* L. with the three species co-existing at 1:1:1 ratio formed the plant community. Drier areas (elevation levels of 50.45-50.60 m) were mostly colonized by dry meadow species such as *Poa* spp. and *Calamagrostis* spp., including patches dominated by *Cirsium* species (Fig. S1).

2.2 Water and micrometeorological measurements

Water monitoring stations were set up at the inlet (60.3283° N, 24.3356° E) and at the outlet (60.3281° N, 24.3377° E) of the wetland. During the 2012-2013 and 2013-2014 monitoring periods, water temperature as well as water turbidity, oxygen concentration, conductivity and pH were measured at the inlet and outlet monitoring station with the YSI-6000 series multiparameter sonde (YSI Inc., Yellow Springs, OH, USA). Measurements were conducted continuously with 10-minute interval. Water level at the outlet was measured continuously with a pressure gauge (STS sensor, Sensor Technik Sirnach AG, Switzerland). At the outlet monitoring station, the concentration of dissolved carbon dioxide ($[CO_2]$) and dissolved methane ($[CH_4]$) were measured with Contros HydroC™ CO_2 and HydroC™ CH_4 sensors (CONTROS Systems

https://doi.org/10.5194/bg-2019-279
Preprint. Discussion started: 18 September 2019

& Solutions GmbH, Germany). In 2014, the same sensors were also installed at the inlet monitoring station to measure [CO_2] and [CH_4]. Dissolved CO_2 and CH_4 molecules diffuse from water column into the detection chamber through a thin-film composite membrane where the concentration of CO_2 and CH_4 is determined by means of IR absorption spectrometry and Tunable Diode Laser Absorption Spectroscopy, respectively.

Local weather conditions were recorded with a Vaisala WXT weather transmitter (WXT520, Vaisala Oyj, Finland) at the inlet monitoring station. Rainfall, wind speed and direction, temperature and relative humidity were recorded continuously at 10-minute interval. Photosynthetic photon flux density (PPFD) was measured with a PQS1 PAR quantum sensor (Kipp & Zonen, the Netherland). Due to instrument failure we obtained PPFD data only from 26 Jan to 7 April and from 22 July to 29 Dec 2013. The gaps were filled with PPFD data from another meteorological station nearby (60°38' N, 23°58' E) in Lettosuo, Finland. The prevailing wind directions were southwest and northeast, and the average of half-hourly average wind speed was 1.13 m s^{-1} from January to December 2013 with higher wind speed in winter than in summer. The average daily air temperature was 5.9 ℃ with the minimum and maximum daily temperatures of -24.4 ℃ and 23.3 ℃ in year 2013. During the winter 2012-2013, there was ice coverage from the beginning of December 2012 to the end of March 2013. In contrast, winter was mild and warm in 2014 and there was practically no snow cover during a winter period (December 2013-March 2014).

2.3 Greenhouse gas measurements by EC tower and gap-filling

To understand the whole-ecosystem exchange of CO_2 and CH_4 in the wetland, a 2.9 m eddy covariance tower was established in the autumn of 2012 on the southern side of the wetland. The operational period of the EC tower was the entire calendar year of 2013 (from 1 January to 31 December 2013) and the peak growing season in 2014 (from 1 June to 31 August 2014). The EC set-up included a 3D-sonic anemometer (uSonic-3, Metek, Elmshorn, Germany) to measure the three wind speed components and sonic temperature, a gas analyser (LI-7200, Li-Cor Inc., Lincoln, Nebraska, USA) which measures CO_2 and H_2O mixing ratio and a TDL gas analyser (TGA100A, Campbell Scientific Inc., USA) to measure CH_4 mixing ratio. Data from the analyzers were collected on a computer at the frequency of 10 Hz. The post-processing of the EC flux data has been done with EddyUH post-processing software (Mammarella et al., 2016). The fluxes were calculated as 30-min covariances between the vertical wind velocity and the gas mixing ratio using block averaging. The raw data was despiked according to standard methods (Vickers and Mahrt, 1997). Coordinate rotations were conducted by performing a two-step rotation to make the x-axis along the mean wind direction and the mean vertical wind velocity zero within each 30-min block. The time lag between the anemometer and gas analyzer signals, resulting from the transport through the inlet tube, were determined for each 30-min interval by maximizing the cross-correlation function between vertical wind speed and the scalar (CO_2 and CH_4). The fluxes were corrected for high-frequency loss due to the limited frequency response of the EC system and low-frequency loss due to the limited averaging time period used for calculating the fluxes. Theoretically and experimentally determined co-spectral transfer functions at low and high frequency were used in the correction (Mammarella et al., 2009).

After calculating the fluxes, data collected from periods when sonic anemometer showed sign of freezing (mean temperature < 0.5 °C and standard deviation of temperature > 1.5 °C) were discarded. The data collected during weak turbulence with friction velocity below 0.1 m s^{-1} have been removed. The measurement points with flux stationarity greater than 1 were omitted to ensure the quality of the co-variances. Fluxes were further filtered according to the wind direction. Since the patchy forest to the southeast of the EC tower (from 100° to 200°) and the highway to the west (from 200° to 280°) could potentially lead to flow distortion and additional source of CO_2 and CH_4, only fluxes from 280° to

https://doi.org/10.5194/bg-2019-279
Preprint. Discussion started: 18 September 2019

100° were accepted for further analysis. The percentage of 30-min fluxes excluded from this analysis was 72 % for CO_2 and 73 % for CH_4 in 2013, whereas in 2014 the percentage for data exclusion was 54 % for CO_2 and 68 % for CH_4.

We used an artificial neural network (ANN) technique to gap-fill half-hourly flux data using meteorological variables (Moffat et al., 2007;Papale et al., 2006). Those variables included radiation, air temperature, water temperature, water level, wind speed, relative humidity, time of the day, season, and dissolved CO_2 and CH_4 concentration in the water. We tested the model performance with different ANN architectures, starting from the architecture with the most complexity, then reduced the variables to find the simplest ANN architecture with good performance (more than 5 % loss in model accuracy with additional variable reduction). For CO_2, water level and wind speed were found to have trivial contribution to the ANN model thus they were removed from the model input, while for CH_4, only wind speed was removed for the same reason. We found that dissolved gas concentration greatly improved the model prediction as they captured the variation of diffusive fluxes from the water (Fig. S2). Ancillary meteorological variables in general had good data coverage and short gaps (up to several hours) were gap-filled by linear interpolation. The only exception was dissolved gas concentration, which had long measurement breakage in year 2013 (day of year 214-254). Fluxes were therefore gap-filled with two separate ANNs, one with dissolved gas concentration and one without. During the above mentioned period with long gaps, the ANN modeled without dissolved gas concentration were used to gap-fill.

Levenberg-Marquardt algorithm was used in the learning process of ANN. The optimized number of neurons in the hidden layer were determined by training the network 100 times with varying number of neurons (from 3 to 15), and 10 neurons was considered to be sufficient after evaluating the performance of the network using root-mean-square-error (RMSE) (data not shown). The entire dataset was divided into three parts, 2/3 of the data was used to train the networks, 1/6 for testing the networks and the remaining 1/6 was used for validating the networks. Since the training of the networks can be biased towards periods with greater data coverage (e.g. daytime conditions), the environmental variables were first divided into five natural clusters using a k-mean clustering algorithm in Matlab (MATLAB 2015a, The MathWorks, Inc., Natick, Massachusetts, United States), and then the data used for training, testing and validation was proportionally extracted from each cluster. After each data extraction, the network was reinitialized for 10 times to avoid local minima and the initialization with the lowest RMSE was selected and resulting network was saved. We repeated the whole process of data extraction and initialization for 20 times, and we used the median of these 20 predictions to gap-fill the missing flux values. The uncertainty of the ANN gap-filling procedure was presented using a 95 % confidence interval of the 20 ANN predictions.

The gap-filled net ecosystem exchange (NEE) can be further partitioned into two components gross ecosystem production (GEP) and ecosystem respiration (R_{eco}) according to the following equation:

$$NEE = GEP + R_{eco,} \quad (1)$$

where positive R_{eco} represents a net carbon flux from the ecosystem to the atmosphere and negative GEP represents a net carbon input from the atmosphere to the ecosystem. Thus the negative NEE indicates that the ecosystem is a carbon sink and the positive NEE means the ecosystem is a carbon source. R_{eco} was estimated using a model describing the temperature dependence of R_{eco}

$$R_{eco} = R_0 \, e^{[E\left(\frac{1}{T_0} - \frac{1}{T_{air} + T_1}\right)]} \quad (2)$$

where E =346.37 K is an activation-energy-related physiological parameter, T_{air} is the air temperature, T_0 = 56.02 K and T_1= 227.13 K (Lloyd and Taylor, 1994;Aurela et al., 2009). R_0 is the rate of ecosystem respiration at 10 °C. We first fitted

https://doi.org/10.5194/bg-2019-279
Preprint. Discussion started: 18 September 2019

the model with nighttime NEE (which represents the nighttime ecosystem respiration since photosynthesis is assumed to be zero at night) and determined *E*. We then calculated R_0 for each of the bi-weekly periods (Aurela et al., 2009). This model was then extrapolated to daytime periods so that R_{eco} in the daytime was obtained. GEP was estimated as the difference between NEE and R_{eco}.

2.4 Diffusive gas exchange

We calculated diffusive gas exchange *F* from open water according to the boundary layer model

$$F = k\left(c_{aq} - c_{eq}\right), \quad (3)$$

where *k* is the gas transfer velocity (cm h^{-1}), c_{aq} is the gas concentration in surface water (mol m^{-3}) and c_{eq} is the gas concentration that surface water would have when it reaches equilibrium with the air (mol m^{-3}). c_{aq} and c_{eq} can be obtained according to the solubility of the gas

$$c_{aq} = 10^{-3}\, k_H\, p\chi_{water} \quad (4)$$

$$c_{eq} = 10^{-3}\, k_H p\chi_{air} \quad (5)$$

where k_H is Henry's law constant for the respective gas (mol L^{-1} atm^{-1}), *p* is air pressure (atm), χ_{water} is the gas mixing ratio in surface water (ppm) and χ_{air} is the gas mixing ratio in the air (ppm). In this study, χ_{water} was obtained from outlet monitoring station as it was located most time in the flux footprint area and it had longer data coverage than from inlet monitoring station. The gas transfer velocity *k* can be calculated as the formula below (Cole and Caraco, 1998):

$$k = (2.07 + 0.215\, U_{10}^{1.7})\left(\frac{S_c}{600}\right)^{-0.5}, \quad (6)$$

where U_{10} is the horizontal wind speed extrapolated to 10 m using the theoretical log wind profile equation (m s^{-1}, approximately $U_{10} = 1.15\, U$ where *U* is the measured wind speed at 2.9 m height in the study site) and S_c is the temperature-dependent Schmidt number of the respective gas. When gas concentration measurement was not available, linear interpolation was applied to obtain monthly and annual diffusive GHG fluxes from the open water.

Although the above-mentioned Cole-Caraco (CC) method is the most simple and most often used model for gas transfer velocity, the limitation of CC method is that it considers wind as the sole factor to cause the water turbulence and to drive the gas exchange. More complicated models were suggested to include the effect of buoyancy flux driven turbulence (Heiskanen et al., 2014;Tedford et al., 2014). It is important to note that we should apply with caution the model parameterization concluded from other sites with different meteorological and environmental condition. In the present study, the open water is connected shallow open-water pools with a maximum depth of 2 m while other studies are for deeper waters. Meanwhile, recent study showed good agreement between the diffusive fluxes calculated using CC methond and measurements based on floating chamber (Cole et al., 2010).

2.5 Estimating zone fluxes and radiative forcing

By combining EC tower and diffusive flux from the open-water, the following model can be derived

$$F_{EC} = F_{water} \times f_{water} + F_{water} \times f_{water} \quad (7)$$

https://doi.org/10.5194/bg-2019-279
Preprint. Discussion started: 18 September 2019

where F_{EC} is the flux measured by EC tower, F_{water} and F_{veg} stands for the flux from open-water and vegetated area, respectively, f_{water} and f_{veg} are the footprint-weighted spatial fraction of open-water and vegetated area. In this study, ebullition was neither measured nor calculated, so the flux from water was only represented by the diffusive flux.

Specifically, we first modelled the half-hourly flux footprint with a parameterization of a three-dimensional backward Lagrangian footprint model (Kljun et al., 2015) in Matlab (MATLAB 2015a, The MathWorks, Inc., Natick, Massachusetts, United States). Periods in which the wind came from the patchy forest to the southeast of the EC tower (between 100° and 200°) and the highway to the west (between 200° and 280°) were eliminated in the footprint analysis. Secondly, a land cover classification map of vegetated and open-water zones was delineated manually using a high-resolution aerial image acquired from National Land Survey of Finland during the growing season of 2013 (open source: https://www.maanmittauslaitos.fi/) with an image manipulation software (Gimp 2.10.6). Thirdly, the flux footprints were aligned and combined with the land cover classification map to calculate half-hourly f_{veg} and f_{water} within 90 % footprint contour lines. Specifically, we assigned each footprint pixel within the 90 % footprint area to either open-water or vegetated area on the land cover classification map while the footprint of the pixels outside 90 % footprint area were regarded as zero. f_{water} was calculated as the sum of footprint within open-water area to the total footprints while f_{veg} was calculated as the sum of footprint within vegetated area to the total footprints. Noting that none of the 90 % footprint contour lines exceeded the map area, the sum of f_{veg} and f_{water} equaled to 1. In order to obtain the long-term aggregated footprint of carbon fluxes, we calculated also the monthly and annual aggregated footprint climatology during the study period.

To better understand the influence of greenhouse gas fluxes in this urban wetland, we calculated the sustained global warming potential (SGWP) for CO_2 and CH_4 over a hundred-year horizon in each surface type. The difference between SGWP and global warming potential (GWP) is that SGWP accounts for the effect of GHG remains in the atmosphere during the period. Since CH_4 is a more potent greenhouse gas, we multiply the emission of CH_4 by a factor of 45 to convert it to kg CO_2-eq m^{-2} yr^{-1} (Neubauer and Megonigal, 2015).

2.6 Statistical analysis

The Pearson correlations (r) were determined between fluxes and environmental variables. Differences in the fluxes and environmental variables between the two peak growing seasons (summer 2013 and 2014) were evaluated using the t-test. Cumulative annual GHG fluxes measured by EC tower are reported as the median of the 20 ANN predictions and uncertainty are presented as 95 % confidence interval of the 20 ANN predictions. As diffusive GHG fluxes were calculated from gas concetration meteorological parameters, no standard error is reported for the cumulative annual fluxes from the open water. All statistical analysis were performed in Matlab (MATLAB 2015a, The MathWorks, Inc., Natick, Massachusetts, United States).

3 Results

3.1 Ecosystem seasonality and environmental variables

Daily average PPFD ranged from 0.9 to 691.5 µmol m^{-2} s^{-1} in year 2013 with the highest value appeared in July. June had the highest monthly average PPFD with 486.1 µmol m^{-2} s^{-1} followed by July and August with 470.2 and 430.6 µmol m^{-2} s^{-1}, respectively. The PPFD during the peak growing season in year 2014 was on average 361.8 µmol m^{-2} s^{-1}, lower than that during the same period in 2013 (Fig. 1a).

https://doi.org/10.5194/bg-2019-279
Preprint. Discussion started: 18 September 2019

Mean daily water temperature (T_{water}) ranged from 0 °C in March to 23.7 °C in June with an annual average of 7.9 °C in 2013 and from 0 °C in February to 21.4°C in July in 2014. Mean daily air temperature (T_{air}) had more fluctuation and ranged from -15.6 °C in January to 23.3 °C in June 2013 and from -19.0 °C in January to 23.4 °C in July 2014 (Fig. 1b). The open-water area experienced an ice-covered period between 1 January and 31 March 2013, while the winter 2013-2014 was so mild and warm that there was practically no snow cover during December 2013 – March 2014. Comparing the temperature between the two peak growing seasons, both T_{water} and T_{air} were higher in June 2013 while T_{air} was lower in July 2013 than in 2014. In August, there was no significant temperature difference between the two years. Four seasons were classified for the ecosystem based on the trend in T_{air} and T_{water}. In spring (April and May), the daily temperature started to increase, the vegetation showed a sign of early growing season and the warm temperature unfroze the lake. In summer, the peak growing season (June - August), vegetation exhibited the maximum growth which was reflected in the large negative GEP value, and the temperatures reached the annual maxima. In autumn (September and October), daily temperatures began to drop and the vegetation showed signs of early senescence. In winter (January to March and November, December), temperatures reached the annual minima and vegetation was inactive in carbon sequestration. Precipitation was higher in August 2014 than in the preceding August, almost twice as high as that of 2013.

WL was higher in the winter and lower in the summer in 2013. The daily average of WL varied between 50.06 m in July 2013 and 50.4 m in April 2013. There was a spring peak in 2013 when the highest WL was observed due to snow melt while in 2014 no such event appeared due to the mild winter 2013-2014 without ice-covered period (Fig. 1c). The average daily WL from January to August was similar (50.13 cm and 50.15 cm for 2013 and 2014, respectively). However, during peak growing season, it was on average 5.7 cm higher in 2014 than in 2013.

The annual rainfall in 2013 (snowfall not included) was 363.6 mm which happened mostly during summer and autumn (Fig. 1d). The maximum daily-averaged rainfall was in August (26.7 mm day^{-1}) while monthly-averaged rainfall was highest in November with 73.8 mm $month^{-1}$ followed by August with 68.3 mm $month^{-1}$. In 2014, exceptionally high amount of rainfall was observed in August (125.7 mm $month^{-1}$), while the amount of rainfall in the other months were similar to 2013.

The daily-averaged CO_2 concentration in the water ($[CO_2]$) in 2013 had large variation with the maximum (9324 ppm) and the minimum (353 ppm) both happening in October (Fig. 1e). $[CO_2]$ was higher in summer months (5457 ppm) and lower in winter months (3345 ppm). $[CO_2]$ was higher in 2014 with an average of 4924 ppm from January to August than in 2013 with an average of 3781 ppm. It also exhibited seasonal variation with high concentration in summer (8084 ppm) and low concentration in winter (3513 ppm). The $[CO_2]$ measured in the inflow was generally lower than that in the outflow and they were well correlated (r=0.84). $[CH_4]$ in the outflow was on average five times higher in 2014 than in 2013. The average annual concentration was 0.81 µmol L^{-1} in year 2013 and 2.25 µmol L^{-1} in 2014. There were peak $[CH_4]$ episodes in the outflow in May 2013 with a maximum of 5.43 µmol L^{-1}. During the summer months in 2014 there were even higher outflow $[CH_4]$ peaks with a maximum of 16.83 µmol L^{-1}. The $[CH_4]$ had a mean of 0.42 µmol L^{-1} in the inflow which was lower than that in the outflow, and there was no prominent $[CH_4]$ peaks observed in the inflow. $[CH_4]$ in the inflow and outflow were weakly correlated (r = 0.2) (Fig. 1f).

3.2 Flux footprint mapping

A footprint distribution was modeled for each half hour when an eddy flux measurement was collected at the EC tower. The open-water area accounted for 10 % to 16 % of the total wetland area within the footprint while the rest was comprised

https://doi.org/10.5194/bg-2019-279
Preprint. Discussion started: 18 September 2019

of wetland vegetation. When weighted with footprint distribution, f_{water} ranged from 0 to 25.5 % and f_{veg} from 74.5 % to 100 %. The 1st quantile, median and 3rd quantile of f_{water} and f_{veg} were 0.09 %, 14.1 %, 17.9 % and 82.1 %, 85.9 %, 91.3 %, respectively.

The monthly cumulative footprint was slightly different for CO_2 and for CH_4 due to the different missing flux values. However, the difference on average was so small (7 %) and the footprint of CO_2 was used in further analysis. The flux footprints were shown to be northeast to the EC mast due to the wind direction filtering meaning only half-hourly data with wind directions from the wetland area were considered in the analysis (Fig. S3). The monthly-average of the 90 % footprint area covered a minimum of 0.69 ha to a maximum of 2.28 ha with a mean of 1.3 ha. The mean extent of the 90 % flux footprints was 128 m. After applying flux footprint function, the monthly-average of the footprint-weighted spatial fraction of open water showed lower value in summer and higher value in winter ranging from 11.3 % to 21.4 % with a mean of 13.3 % in 2013. In 2014 during the peak growing season, on average 13.8 % of the wetland area was comprised of open water and the mean f_{water} was 10 %.

3.3 CO_2 and CH_4 fluxes

3.3.1 Ecosystem CO_2 and CH_4 fluxes

Ecosystem CO_2 and CH_4 fluxes measured by EC tower showed the ecosystem was nearly CO_2 neutral and it was a small CH_4 source in year 2013.

Daily average of NEE was near zero during winter time (January to March, on average 0.37 µmol C-CO_2 m^{-2} s^{-1}), slightly positive in spring and it became negative from the end of May till the end of August indicating the ecosystem was a CO_2 sink during this period, with a maximum negative value of -5.14 µmol C-CO_2 m^{-2} s^{-1} in June. Daily-average NEE was highest in September with a maximum of 3.29 µmol C-CO_2 m^{-2} s^{-1}, possibly due to the suppressed GEP and high R_{eco}. In October, November and December, NEE remained low but still positive (on average 0.77 g µmol C-CO_2 m^{-2} s^{-1}), demonstrating the milder winter between 2013 and 2014 (Fig. 2 and Fig. S4). NEE, GEP and R_{eco} exhibited strong seasonality in 2013 NEE was negative during June, July and August meaning the ecosystem was a CO_2 sink while the rest of year it was a CO_2 source. NEE was lowest in June and highest in September. Both GEP and R_{eco} achieved their highest values in July (Fig. S4). The cumulative NEE in 2013 was 8 g C-CO_2 m^{-2} yr^{-1} with the 95% confidence interval between -18.9 and 34.9 g C-CO_2 m^{-2} yr^{-1} (Fig. 2).

Daily-averaged CH_4 was low but not negligible from January to April (on average 5.1 nmol C-CH_4 m^{-2} s^{-1}), with a sudden rise in the end of May reaching a maximum of 48.9 nmol C-CH_4 m^{-2} s^{-1}. During summer months the ecosystem exhibited relatively high CH_4 emission (on average 15.4 nmol C-CH_4 m^{-2} s^{-1}), not comparable with the emission episode in May but higher than winter months. In autume (September and October) the daily-average CH4 was 8.8 nmol C-CH_4 m^{-2} s^{-1} and after that it gradually decreased throughout the rest of the year with an average of 5.5 nmol C-CH_4 m^{-2} s^{-1}. The cumulative CH_4 for 2013 was 3.9 g C-CH_4 m^{-2} yr^{-1} with the 95% confidence interval between 3.75 and 4.07 g C-CH_4 m^{-2} yr^{-1} (Fig. 3).

Comparing the peak growing season between 2013 and 2014, the 30 mins NEE ranged from -20.0 µmol C-CO_2 m^{-2} s^{-1} in June to 18.5 µmol C-CO_2 m^{-2} s^{-1} in September 2013. GEP reached maximum negative value in July 2013 with -30.5 µmol C-CO_2 m^{-2} s^{-1} and R_{eco} in June with 13.9 µmol C-CO_2 m^{-2} s^{-1}. During the peak growing season 2014, NEE had lowest value -22.6 µmol C-CO_2 m^{-2} s^{-1} in June, GEP -28.6 µmol C-CO_2 m^{-2} s^{-1} and R_{eco} had its maximum in the beginning of August 2014 with 11.3 µmol C-CO_2 m^{-2} s^{-1}. The monthly NEEs of peak growing season were -84.1, -76,1 and -22.2 g C-

https://doi.org/10.5194/bg-2019-279
Preprint. Discussion started: 18 September 2019

CO_2 m^{-2} $month^{-1}$ in June, July and August 2013, and -97.6, -47,5 and -19.6 g C-CO_2 m^{-2} $month^{-1}$ in 2014. In both years, daily-averaged GEP had its maximum negative value in July (-13.4 and -12.8 g C-CO_2 m^{-2} d^{-1}). Daily-averaged R_{eco} was highest in June 2013 with 12.1 g C-CO_2 m^{-2} d^{-1} while in 2014 R_{eco} was low in June and the peak was in the end of July with 10.5 g C-CO_2 m^{-2} d^{-1} (Fig. S5a). The average CH_4 emission in June, July and August were 24.4, 10.8 and 11 nmol m^{-2} s^{-1} in 2013, and 15.5, 21.3 and 21.3 nmol m^{-2} s^{-1} in 2014, respectively (Fig. S5b).

3.3.2 Diffusive CO_2 and CH_4 fluxes from open-water area

Diffusive CO_2 and CH_4 fluxes from the open water were estimated based on wind speed, [CO_2] and [CH_4] (See Sect. 2.4). The variation of diffusive fluxes demonstrated a pattern driven by both wind speed in short term and gas concentration dynamics in the water in long term. Diffusive CO_2 fluxes ranged from -0.07 to 4.09 µmol CO_2 m^{-2} s^{-1} with a mean of 1.04 µmol CO_2 m^{-2} s^{-1} in 2013 indicating CO_2 oversaturation in the water. From June to September the averaged flux (1.27 µmol CO_2 m^{-2} s^{-1}) was higher than that of the other months (Fig. 4a), corresponding to the higher [CO_2] in the water during summer months (Fig. 1d). The monthly-averaged diffusive CO_2 flux during peak growing season in 2014 was 2.34, 2.71 and 1.99 µmol CO_2 m^{-2} s^{-1} for June, July and August, significantly higher than during the same period in 2013 due to the high [CO_2] in the open water (Fig. 1d).

The average diffusive CH_4 emissions in 2013 was 4.9 nmol C-CH_4 m^{-2} s^{-1}, where a peak emission appeared in late May with the highest flux of 137.6 nmol C-CH_4 m^{-2} s^{-1}. Monthly-averaged CH_4 diffusive fluxes showed an increasing trend towards the end of the year with large variation in May due to the peak concentration episode. This phenomenon was mainly driven by the increasing dissolved CH_4 concentration in the outflow in 2013. The monthly-averaged diffusive CH_4 flux during peak growing season in 2014 was 20.9, 18.9 and 13.5 nmol CH_4 m^{-2} s^{-1} for June, July and August, respectively and they were significantly higher than the same period in 2013 due to the high [CH_4] in the open water (Fig. 1e).

3.3.3 Diel patterns in CO_2 and CH_4 fluxes

Only non-gapfilled data were used for determination of diel patterns in both gas fluxes. CO_2 and CH_4 fluxes from vegetated area (F_{veg}) was calculated for each 30-min interval according to formula (5). As expected, CO_2 flux showed strong diel pattern in summer with CO_2 uptake during daytime and release in the night, which was controlled by photosynthetic activity (Fig. 5a). The summer peak CO_2 uptake reached 11.5 µmol m^{-2} s^{-1} for the whole constructed wetland ecosystem and 15.2 µmol m^{-2} s^{-1} for the vegetated area. The CO_2 flux from the vegetated area had higher maximum uptake than the EC measurements carried out over the whole constructed wetland. In the winter, the CO_2 fluxes from both tower and vegetation were similar, being on average 0.46 and 0.55 µmol m^{-2} s^{-1} respectively (Fig. 5b).

CH_4 flux also showed diel patterns in the summer with much larger variability than those from CO_2 flux. CH_4 emission in general was higher in daytime than in nighttime. In the daytime in summer, CH_4 flux from the vegetated area was higher than the flux measured from the tower while there was no difference during the nighttime (Fig. 5c, 5d). The summer peak daytime flux from tower (18.9 nmol m^{-2} s^{-1}) and vegetated area (24.7 nmol m^{-2} s^{-1}) was 2.4 times and 3.3 times higher than the nighttime flux (7.5 nmol m^{-2} s^{-1}), respectively. This can be understood as daytime CH_4 flux is linked with photosynthesis while nighttime CH_4 flux is controlled by other processes like diffusion, ebullition and convection between the soil, water and atmosphere. In winter there was small (on average 4.6 nmol m^{-2} s^{-1}) but constantly positive CH_4 flux without obvious diel pattern.

3.4 Environmental variables with fluxes

https://doi.org/10.5194/bg-2019-279
Preprint. Discussion started: 18 September 2019

Only non-gapfilled flux data were used in the Pearson correlation analysis between environmental variables and flux pairs. Radiation, T_{air} and T_{water} all had high negative correlation coefficient (*r*) with NEE and high positive *r* with CH_4 flux in 2013, corresponding to the results of ANN model parameter selection. Radiation was best correlated with NEE and T_{water} was best correlated with CH_4 (Table 1). The correlations were rather weak (small *r* or even the opposite sign of *r*) during 2014 due to the short measuring period and narrow ranges of the variables. Water level was positively correlated with NEE and negatively correlated with CH_4, which was counter intuition, possibly because it was masked by temperature variation as the water level was in general higher in winter and lower in summer. [CO_2] and [CH_4] were not correlated with either NEE or CH_4 although they were shown to be important parameters in ANN model selection.

3.5 Estimating radiative forcing from different zones

To obtain the climate forcings from each land surface type, we calculated the half-hourly and annual gas fluxes from the vegetated area based on eq. (7) using footprint-weighted spatial fraction, ecosystem fluxes and diffusive fluxes from the open water (See Sect. 2.5). The annual median value of footprint-weighted spatial extent was used to calculate the annual fluxes, which showed open-water area was a CO_2 source (297.5 g C-CO_2 m^{-2} yr^{-1}) and vegetated area was a CO_2 sink (-39.5 C-CO_2 m^{-2} yr^{-1}). Both open-water and vegetated area were CH_4 sources but the CH_4 emission from vegetated area was higher than open-water area, being 4.26 and 1.73 g C-CO_2 m^{-2} yr^{-1}, respectively (Table 2).

Open water has contributed large amount of CO_2 emission into the atmosphere through diffusion (1.09 kg CO_2-eq m^{-2} yr^{-1}) whereas the CH_4 emission was relatively small (0.104 kg CO_2-eq m^{-2} yr^{-1}). Vegetated area was a small sink of CO_2 but the cooling effect of vegetation by CO_2 uptake was relatively small (-0.145 kg CO_2-eq m^{-2} yr^{-1}) compared to its CH_4 emission (0.256 kg CO_2-eq m^{-2} yr^{-1}). Overall, the ecosystem had a small warming effect with 0. 263 kg CO_2-eq m^{-2} yr^{-1} of which 89% was contributed by CH_4 (Table 2).

4 Discussion

4.1 The GHG fluxes from an urban stormwater wetland ecosystem

The studied urban wetland ecosystem was a small carbon source over the full-year studied period in year 2013. Due to the scarcity of studies on urban wetlands using the EC method, we compare our results to restored wetlands which can be considered to be proxy ecosystems to urban wetlands with both including rewetting practice in an ecosystem which has been drained previously. The annual CO_2 balance of 8 g C-CO_2 m^{-2} yr^{-1} from the ecosystem, or -39.5 g C-CO_2 m^{-2} yr^{-1} from the vegetated area (Table 2), were small compared to a restored wetland in western Denmark where the annual CO_2 balance ranged from -286 to -53 g C-CO_2 m^{-2} yr^{-1} (Herbst et al., 2013), and the annual CH_4 balance of 3.9 g C-CH_4 m^{-2} yr^{-1} was less than half of the annual CH_4 emission (between 9 and 13 g C-CH_4 m^{-2} yr^{-1}) in that study. Over a network of restored freshwater wetlands in the California, the CO_2 sequestration can be up to nearly 700 g C m^{-2} yr^{-1} and CH_4 emission up to 63 g C m^{-2} yr^{-1} (Hemes et al., 2018). It is not surprising that the studied ecosystem appeared to CO_2 neutral as it was recently constructed. The herbaceous vegetation has been allowed to fully self-establish without human intervention and at the early successional stage, plant diversity and biomass were still increasing each year (Wahlroos, 2019). With the vegetation being more developed, a greater CO_2 uptake from the vegetated area can be expected in the following years. The low CH_4 emission observed in this study may be due to the depletion of organic matters in the bottom soil from agricultural uses thus it provided little substrate for anaerobic microbial activity to produce CH_4. With the accumulation of organic matters in the anoxic wetland sediment, CH_4 production may increase in the future. Certain chemical

https://doi.org/10.5194/bg-2019-279
Preprint. Discussion started: 18 September 2019

compounds like Fe in mineral soils can also inhibit CH_4 production leading to much lower ecosystem-scale CH_4 flux (Chamberlain et al., 2018). In the meanwhile, methane-oxidizing bacteria (methanotroph) regulates CH_4 consumption at the soil-water interface. With the ecosystem being used previously as cropland, the physical disturbance of soil may have greatly reduced the methanotroph communities so that the CH_4 oxidation may also be low in the soil (Smith et al., 2000;Saggar et al., 2008). Furthermore, after the initial establishing phase, the ecosystem productivity can also be reduced due to the standing litter that inhibits the generation of new vegetation growth. It was shown that in a restored freshwater wetland the ecosystem was a net CO_2 sink (-804 ± 131 g C-CO_2 m^{-2} yr^{-1}) in 2002-2003, six years after the restoration but near CO_2 neutral in 2010-2011 due to the reduced photosynthetic plants (Anderson et al., 2016). Thus, given the urban wetland is sustained for a sufficiently long period, it is still unclear whether the CO_2 uptake from vegetated zone would compensate its CH_4 emission, not considering the large GHG emission from the open-water zone. Thus, similar studies as the present one should be conducted at a later stage after the construction of the wetland to fully reveal the GHG balance of the ecosystem along time.

Overall, the ecosystem CO_2 and CH_4 fluxes measured by EC tower ranged from -5.33 to 3.4 g C-CO_2 m^{-2} day^{-1} and from 1.0 to 55.2 mg C-CH_4 m^{-2} day^{-1}, respectively. They are consistent with the flux ranges provided by other studies on GHG fluxes in restored wetlands (Anderson et al., 2016;Knox et al., 2015;Matthes et al., 2014;Morin et al., 2014b;Herbst et al., 2013), although for both gases they tend to be on the lower end. NEE, GEP and R_{eco} exhibited seasonal variation so that the ecosystem was a CO_2 sink between June and August. The highest NEE appeared in September possibly because GEP has greatly reduced due to plant senescent while R_{eco} remained relatively high because of the warm temperature (Fig. S4). Previous studies have found good agreement between CH_4 emission and GEP as plants provide substrates for methanogenesis (Rinne et al., 2018), which was not observed in the daily-average of gas fluxes in this study (Figs 2 and 3) as the peak CH_4 flux appeared in May and peak GEP appeared in July. Nonetheless, both CH_4 and CO_2 fluxes, especially those obtained from vegetated area, exhibited strong diurnal cycle during summer with synchronized peaks around noon (Fig. 5a, 5c). This finding reflects that short-term CH_4 emission from vegetation is linked with photosynthesis by providing labile carbon from root exudate and by gas transport through aerenchyma and open stomata while long-term CH_4 emission may be determined by complex processes related to environmental variables e.g. temperature and redox potential (Linden et al., 2014).

4.2 Parsing GHG fluxes from heterogeneous land surfaces

We found the open-water area was constantly a source of CO_2 and CH_4 to the atmosphere during the studied period as the [CO_2] and [CH_4] in the water generally exceeded the atmosphere equilibrium except the ice-covered period (Fig. 4). The annual average of [CO_2] in the surface water in 2013 was 0.3% in our study, comparable to 0.4% in another temperate restored wetland (McNicol et al., 2017), while the seasonal pattern (higher in summer and fall) was the opposite as they have found. We also found that both [CO_2] and [CH_4] were higher in 2014 than 2013 (Fig. 1d, 1e). The O_2 concentration ([O_2]) and O_2 balance ($[O_2]_{outlet}$ - $[O_2]_{inlet}$) measured by another study on the same wetland (Wahlroos, 2019) could partially explain the observed phenomenon. The relatively high water temperature and oxic conditions in the water in fall 2013 have allowed high decomposition of detritus leading to high [CO_2] (Wahlroos, 2019). The long period of hypoxia during summer 2014 could explain the three-fold increase in [CH_4] as the condition was more favorable for CH_4 production. The negative O_2 balance in summer 2014 indicated strong O_2 consumption by microbial decomposition producing CO_2 in the water. As the long-term diffusive fluxes (daily and monthly) was mainly driven by gas concentration in the water, it was straight forward to understand high diffusive CO_2 and CH_4 fluxes in 2014 comparing to 2013. Interestingly, the ecosystem

https://doi.org/10.5194/bg-2019-279
Preprint. Discussion started: 18 September 2019

CH_4 emission in 2013 was well synchronized with the diffusive CH_4 flux by capturing sporadic emission episodes from the water (Fig. S6a, S6c) while they were not synchronized in summer 2014 although several stronger diffusive peaks happened (Fig. S6b, S6d). When footprint-weighted contribution was accounted for, it clearly revealed that the synchronization of CH_4 emission from ecosystem and water was closely related to the flux footprint distribution. When there was high flux contribution from the open water (20-25 %), high diffusive CH_4 was also reflected in ecosystem flux measured by EC. This has further proved the application of footprint analysis is essential in explaining gas exchange from heterogeneous surfaces using EC data.

It is worth noticing that in our study we only classified the surface landscapes into "open water" and "vegetation" but neglected the difference in sink/source strength from different plant types within the vegetation zone (Fig. S1). We did not account for the dissimilarity between vegetation types because the characteristics in gas exchange are much more distinct between open water and vegetation, which was the focus of this study. For the same reason, ebullition was not considered in this study neither, as ebullition was shown to have only minor significance in a restored wetland accounting for less than 0.1% of ecosystem CO_2 flux and 4.1% of ecosystem CH_4 flux (McNicol et al., 2017). However, for a proper downscaling analysis of EC data, the subareas of different plant types and ebullition should also be taken into account.

4.3 Climate impact of urban wetland and implications for management

In the present study, the urban boreal wetland had an overall SGWP of 0.263 kg CO_2-eq m^{-2} yr^{-1} which was comparable or higher than other restored wetlands in boreal region (Herbst et al., 2013), and within the range of inter-annual variation or lower than restored wetlands in temperate zone (McNicol et al., 2017;Anderson et al., 2016). Different from other studies, the urban wetland was CO_2 neutral and a CH_4 source. It is worth noting that the paramount contribution of CH_4 in ecosystem SGWP was mainly driven by the large footprint-weighted spatial area of vegetation (See Sect. 3.2). In fact, The SGWP of GHG emission from open water (1.194 kg CO_2-eq m^{-2} yr^{-1}) was 10 times as large as that from vegetation (0.111 kg CO_2-eq m^{-2} yr^{-1}) (Table 2). The implication of this result is that during wetland restoration, it would be more beneficial to have large patches of emergent vegetation area at least from the GHG emission point of view. Similar results have been obtained by other studies as well that open water has more climate-warming impact than emergent vegetation due to the large diffusive fluxes from open water (Stefanik and Mitsch, 2014;McNicol et al., 2017). The climate impact of natural wetland depends on the net balance between the cooling effect of CO_2 uptake by vegetation and the warming effect of other GHG emissions, mainly CH_4 (Bridgham et al., 2013). In wetlands constructed in urban area, the large fraction of open water which is a significant emitter of CO_2, should also be taken into consideration when evaluating the role of urban wetland in global climate change.

5 Conclusions

Urban wetlands have received global attention as a nature-based urban runoff management solution for sustainable cities, as they provide cost efficient flood control and water quality mitigation as well as many ecological and cultural services. In the meantime, the climate impact of urban wetlands should also be considered. Wetting a landscape may enhance the CO_2 sequestration in the ecosystem, whereas CH_4 can be emitted due to the anaerobic conditions in the soil after wetting. Furthermore, heterogeneity induced in newly created urban wetland may contribute differently to the overall climate impact.

https://doi.org/10.5194/bg-2019-279
Preprint. Discussion started: 18 September 2019

In the present study, for the first time a full annual carbon balance of an urban stormwater wetland in the boreal region was evaluated and the radiative forcing from heterogeneous landscapes were presented. We found that, during the monitored period at the study wetland, both the open water area and the vegetated area within the created wetland were carbon sources, and thus the urban wetland had a net climate warming effect, the monitored fourth year after the wetland establishment. The radiative forcing effect of the open-water area exceeded the vegetated area, which indicated that limiting open-water surfaces and setting a design preference for areas of emergent vegetation in the establishment of urban wetlands can be a beneficial practice when considering only the climate impact of a created urban wetland. In the meanwhile, we also emphasize that the value of urban wetlands should not be determined solely by GHG radiative forcing. The values of urban wetlands in other areas e.g. flood control, pollutant removal, biodiversity, recreation and education are as well of paramount importance to human society.

Data availability

Eddy covariance, gas concentration and meteorological data are available from the DRYAD database at https://datadryad.org/stash/share/WrtTNnpIt6FgLoMSZ_Wlr0lK22IcxqjGZAStuuKdHLs

Author contribution

IM, OW, HV, AO and TV designed the field study. SH, IM and JP carried out eddy covariance measurements, automatic gas concentration measurements in the open water and manual field measurements. XL and IM participated in eddy covariance data processing and analysis. XL analysed the results and prepared the manuscript with contributions from all co-authors.

Competing interests

The authors declare that they have no conflict of interest.

Acknowledgments

We thank Mikko Yli-Rosti and Kiril Aspila for assistance for the maintenance of the field measurements. This research was supported by the EU Life+11 ENV/FI/911 Urban Oases project grant, Academy of Finland, Academy Professor projects (312571 and 282842), ICOS-Finland (281255), the Maa- ja vesitekniikan tuki ry, the Ministry of the Environment of Finland and the Municipality of Vihti. In memoriam: The greenhouse gas exchange measurements at the Gateway Wetland were made possible due to the creative and caring support by late Professor Eero Nikinmaa to the Urban Oases project.

References

Anderson, F. E., Bergamaschi, B., Sturtevant, C., Knox, S., Hastings, L., Windham-Myers, L., Detto, M., Hestir, E. L., Drexler, J., Miller, R. L., Matthes, J. H., Verfaillie, J., Baldocchi, D., Snyder, R. L., and Fujii, R.: Variation of energy and carbon fluxes from a restored temperate freshwater wetland and implications for carbon market verification protocols, Journal of Geophysical Research-Biogeosciences, 121, 777-795, 10.1002/2015jg003083, 2016.

Aurela, M., Lohila, A., Tuovinen, J. P., Hatakka, J., Riutta, T., and Laurila, T.: Carbon dioxide exchange on a northern boreal fen, Boreal Environment Research, 14, 699-710, 2009.

Baldocchi, D., Detto, M., Sonnentag, O., Verfaillie, J., Teh, Y. A., Silver, W., and Kelly, N. M.: The challenges of measuring methane fluxes and concentrations over a peatland pasture, Agricultural and Forest Meteorology, 153, 177-187, 10.1016/j.agrformet.2011.04.013, 2012.

https://doi.org/10.5194/bg-2019-279
Preprint. Discussion started: 18 September 2019

542 Baldocchi, D. D.: Assessing the eddy covariance technique for evaluating carbon dioxide exchange rates of
543 ecosystems: past, present and future, Global Change Biology, 9, 479-492, 10.1046/j.1365-
544 2486.2003.00629.x, 2003.
545 Bridgham, S. D., Cadillo-Quiroz, H., Keller, J. K., and Zhuang, Q. L.: Methane emissions from wetlands:
546 biogeochemical, microbial, and modeling perspectives from local to global scales, Global Change Biology,
547 19, 1325-1346, 10.1111/gcb.12131, 2013.
548 Chamberlain, S. D., Anthony, T. L., Silver, W. L., Eichelmann, E., Hemes, K. S., Oikawa, P. Y., Sturtevant,
549 C., Szutu, D. J., Verfaillie, J. G., and Baldocchi, D. D.: Soil properties and sediment accretion modulate
550 methane fluxes from restored wetlands, Global Change Biology, 24, 4107-4121, 10.1111/gcb.14124, 2018.
551 Cole, J. J., and Caraco, N. F.: Atmospheric exchange of carbon dioxide in a low-wind oligotrophic lake
552 measured by the addition of SF6, Limnology and Oceanography, 43, 647-656, 10.4319/lo.1998.43.4.0647,
553 1998.
554 Cole, J. J., Bade, D. L., Bastviken, D., Pace, M. L., and Van de Bogert, M.: Multiple approaches to
555 estimating air-water gas exchange in small lakes, Limnology and Oceanography-Methods, 8, 285-293,
556 10.4319/lom.2010.8.285, 2010.
557 Frolking, S., Roulet, N., and Fuglestvedt, J.: How northern peatlands influence the Earth's radiative budget:
558 Sustained methane emission versus sustained carbon sequestration, Journal of Geophysical Research-
559 Biogeosciences, 111, 10.1029/2005jg000091, 2006.
560 Heiskanen, J. J., Mammarella, I., Haapanala, S., Pumpanen, J., Vesala, T., Macintyre, S., and Ojala, A.:
561 Effects of cooling and internal wave motions on gas transfer coefficients in a boreal lake, Tellus Series B-
562 Chemical and Physical Meteorology, 66, 10.3402/tellusb.v66.22827, 2014.
563 Hemes, K. S., Chamberlain, S. D., Eichelmann, E., Knox, S. H., and Baldocchi, D. D.: A Biogeochemical
564 Compromise: The High Methane Cost of Sequestering Carbon in Restored Wetlands, Geophysical Research
565 Letters, 45, 6081-6091, 10.1029/2018gl077747, 2018.
566 Herbst, M., Friborg, T., Schelde, K., Jensen, R., Ringgaard, R., Vasquez, V., Thomsen, A. G., and Soegaard,
567 H.: Climate and site management as driving factors for the atmospheric greenhouse gas exchange of a
568 restored wetland, Biogeosciences, 10, 39-52, 10.5194/bg-10-39-2013, 2013.
569 Kljun, N., Calanca, P., Rotach, M. W., and Schmid, H. P.: A simple two-dimensional parameterisation for
570 Flux Footprint Prediction (FFP), Geoscientific Model Development, 8, 3695-3713, 10.5194/gmd-8-3695-
571 2015, 2015.
572 Knox, S. H., Sturtevant, C., Matthes, J. H., Koteen, L., Verfaillie, J., and Baldocchi, D.: Agricultural
573 peatland restoration: effects of land-use change on greenhouse gas (CO2 and CH4) fluxes in the Sacramento-
574 San Joaquin Delta, Global Change Biology, 21, 750-765, 10.1111/gcb.12745, 2015.
575 Linden, A., Heinonsalo, J., Buchmann, N., Oinonen, M., Sonninen, E., Hilasvuori, E., and Pumpanen, J.:
576 Contrasting effects of increased carbon input on boreal SOM decomposition with and without presence of
577 living root system of Pinus sylvestris L, Plant and Soil, 377, 145-158, 10.1007/s11104-013-1987-3, 2014.
578 Lloyd, J., and Taylor, J. A.: ON THE TEMPERATURE-DEPENDENCE OF SOIL RESPIRATION,
579 Functional Ecology, 8, 315-323, 10.2307/2389824, 1994.
580 Lucas, R., Earl, E. R., Babatunde, A. O., and Bockelmann-Evans, B. N.: Constructed wetlands for
581 stormwater management in the UK: a concise review, Civil Engineering and Environmental Systems, 32,
582 251-268, 10.1080/10286608.2014.958472, 2015.
583 Mammarella, I., Launiainen, S., Gronholm, T., Keronen, P., Pumpanen, J., Rannik, U., and Vesala, T.:
584 Relative Humidity Effect on the High-Frequency Attenuation of Water Vapor Flux Measured by a Closed-
585 Path Eddy Covariance System, Journal of Atmospheric and Oceanic Technology, 26, 1856-1866,
586 10.1175/2009jtecha1179.1, 2009.
587 Mammarella, I., Peltola, O., Nordbo, A., Jarvi, L., and Rannik, U.: Quantifying the uncertainty of eddy
588 covariance fluxes due to the use of different software packages and combinations of processing steps in two
589 contrasting ecosystems, Atmospheric Measurement Techniques, 9, 4915-4933, 10.5194/amt-9-4915-2016,
590 2016.
591 Mander, U., Dotro, G., Ebie, Y., Towprayoon, S., Chiemchaisri, C., Nogueira, S. F., Jamsranjav, B., Kasak,
592 K., Truu, J., Tournebize, J., and Mitsch, W. J.: Greenhouse gas emission in constructed wetlands for
593 wastewater treatment: A review, Ecological Engineering, 66, 19-35, 10.1016/j.ecoleng.2013.12.006, 2014.
594 Matthes, J. H., Sturtevant, C., Verfaillie, J., Knox, S., and Baldocchi, D.: Parsing the variability in CH4 flux
595 at a spatially heterogeneous wetland: Integrating multiple eddy covariance towers with high-resolution flux

https://doi.org/10.5194/bg-2019-279
Preprint. Discussion started: 18 September 2019

footprint analysis, Journal of Geophysical Research-Biogeosciences, 119, 1322-1339, 10.1002/2014jg002642, 2014.
McNicol, G., Sturtevant, C. S., Knox, S. H., Dronova, I., Baldocchi, D. D., and Silver, W. L.: Effects of seasonality, transport pathway, and spatial structure on greenhouse gas fluxes in a restored wetland, Global Change Biology, 23, 2768-2782, 10.1111/gcb.13580, 2017.
Mitsch, W. J., and Gosselink, J. G.: Wetlands, 5th ed, John Wiley & Sons Inc., Hoboken, NJ, 2015.
Moffat, A. M., Papale, D., Reichstein, M., Hollinger, D. Y., Richardson, A. D., Barr, A. G., Beckstein, C., Braswell, B. H., Churkina, G., Desai, A. R., Falge, E., Gove, J. H., Heimann, M., Hui, D. F., Jarvis, A. J., Kattge, J., Noormets, A., and Stauch, V. J.: Comprehensive comparison of gap-filling techniques for eddy covariance net carbon fluxes, Agricultural and Forest Meteorology, 147, 209-232, 10.1016/j.agrformet.2007.08.011, 2007.
Morin, T. H., Bohrer, G., Frasson, R., Naor-Azreli, L., Mesi, S., Stefanik, K. C., and Schafer, K. V. R.: Environmental drivers of methane fluxes from an urban temperate wetland park, Journal of Geophysical Research-Biogeosciences, 119, 2188-2208, 10.1002/2014jg002750, 2014a.
Morin, T. H., Bohrer, G., Naor-Azrieli, L., Mesi, S., Kenny, W. T., Mitsch, W. J., and Schafer, K. V. R.: The seasonal and diurnal dynamics of methane flux at a created urban wetland, Ecological Engineering, 72, 74-83, 10.1016/j.ecoleng.2014.02.002, 2014b.
Mungasavalli, D. P., and Viraraghavan, T.: Constructed wetlands for stormwater management: A review, Fresenius Environmental Bulletin, 15, 1363-1372, 2006.
Neubauer, S. C., and Megonigal, J. P.: Moving Beyond Global Warming Potentials to Quantify the Climatic Role of Ecosystems, Ecosystems, 18, 1000-1013, 10.1007/s10021-015-9879-4, 2015.
Papale, D., Reichstein, M., Aubinet, M., Canfora, E., Bernhofer, C., Kutsch, W., Longdoz, B., Rambal, S., Valentini, R., Vesala, T., and Yakir, D.: Towards a standardized processing of Net Ecosystem Exchange measured with eddy covariance technique: algorithms and uncertainty estimation, Biogeosciences, 3, 571-583, 10.5194/bg-3-571-2006, 2006.
Pirinen, P., Simola, H., Aalto, J., Kaukoranta, J.-P., Karlsson, P., and Ruuhela, R.: Tilastoja Suomen ilmastosta 1981 - 2010, 2012.
Rinne, J., Tuittila, E. S., Peltola, O., Li, X. F., Raivonen, M., Alekseychik, P., Haapanala, S., Pihlatie, M., Aurela, M., Mammarella, I., and Vesala, T.: Temporal Variation of Ecosystem Scale Methane Emission From a Boreal Fen in Relation to Temperature, Water Table Position, and Carbon Dioxide Fluxes, Global Biogeochemical Cycles, 32, 1087-1106, 10.1029/2017gb005747, 2018.
Saggar, S., Tate, K. R., Giltrap, D. L., and Singh, J.: Soil-atmosphere exchange of nitrous oxide and methane in New Zealand terrestrial ecosystems and their mitigation options: a review, Plant and Soil, 309, 25-42, 10.1007/s11104-007-9421-3, 2008.
Smith, K. A., Dobbie, K. E., Ball, B. C., Bakken, L. R., Sitaula, B. K., Hansen, S., Brumme, R., Borken, W., Christensen, S., Prieme, A., Fowler, D., Macdonald, J. A., Skiba, U., Klemedtsson, L., Kasimir-Klemedtsson, A., Degorska, A., and Orlanski, P.: Oxidation of atmospheric methane in Northern European soils, comparison with other ecosystems, and uncertainties in the global terrestrial sink, Global Change Biology, 6, 791-803, 10.1046/j.1365-2486.2000.00356.x, 2000.
Stefanik, K. C., and Mitsch, W. J.: Metabolism and methane flux of dominant macrophyte communities in created riverine wetlands using open system flow through chambers, Ecological Engineering, 72, 67-73, 10.1016/j.ecoleng.2013.10.036, 2014.
Stocker, T. F., Qin, D., Plattner, G. K., Tignor, M. M. B., Allen, S. K., Boschung, J., Nauels, A., Xia, Y., Bex, V., and Midgley, P. M.: Climate Change 2013: The Physical Science Basis, Climate Change 2013: The Physical Science Basis, edited by: Stocker, T. F., Qin, D., Plattner, G. K., Tignor, M. M. B., Allen, S. K., Boschung, J., Nauels, A., Xia, Y., Bex, V., and Midgley, P. M., 1-1535 pp., 2014.
Tedford, E. W., MacIntyre, S., Miller, S. D., and Czikowsky, M. J.: Similarity scaling of turbulence in a temperate lake during fall cooling, Journal of Geophysical Research-Oceans, 119, 4689-4713, 10.1002/2014jc010135, 2014.
Wahlroos, O., Valkama, P., Mäkinen, E., Ojala, A., Vasander, H., Väänänen, V.-M., Halonen, A., Lindén, L., Nummi, P., Ahponen, H., Lahti, K., and Vessman, T. R., Kari; Nikinmaa, Eero Urban wetland parks in Finland: improving water quality and creating endangered habitats, International Journal of Biodiversity Science, Ecosystem Services & Management, 11, 46-60, 10.1080/21513732.2015.1006681, 2015.
Wahlroos, O.: Life+ Urban Oases final project report, www.helsinki.fi/urbanoases, www.helsinki.fi/urbanoases, 2019.

https://doi.org/10.5194/bg-2019-279
Preprint. Discussion started: 18 September 2019

651 Vasander, H., Tuittila, E. S., Lode, E., Lundin, L., Ilomets, M., Sallantaus, T., Heikkila, R., Pitkanen, M. L.,
652 and Laine, J.: Status and restoration of peatlands in northern Europe, Wetlands Ecology and Management,
653 11, 51-63, 10.1023/a:1022061622602, 2003.
654 Vickers, D., and Mahrt, L.: Quality control and flux sampling problems for tower and aircraft data, Journal
655 of Atmospheric and Oceanic Technology, 14, 512-526,1997.

656

https://doi.org/10.5194/bg-2019-279
Preprint. Discussion started: 18 September 2019

657 **Tables**

658 Table 1. Pearson correlation coefficient (r) between the daily averages of environmental variables and fluxes in year
659 2013 and 2014. NEE – net ecosystem exchange; T_{air} – air temperature; T_{water} – water temperature; PPFD –
660 photosynthetic photon flux density; WL – water level; $[CO_2]$ and $[CH_4]$ – CO_2 and CH_4 concentration measured in the
661 outlet; * indicates only peak growing season (June, July and August) are included in the analysis.

Flux	Year	T_{air}	T_{water}	PPFD	WL	$[CO_2]$	$[CH_4]$
CO_2	2013	-0.45	-0.61	-0.62	0.46	-0.34	0.18
	2014	0.43	0.54	-0.12	0.12	-0.12	-0.05
CH_4	2013	0.61	0.65	0.56	-0.3	0.17	-0.09
	2014*	0.37	0.26	0.27	-0.24	0.28	0.25

662

663

https://doi.org/10.5194/bg-2019-279
Preprint. Discussion started: 18 September 2019

664 Table 2. Annual CO_2 and CH_4 exchange from different surface zones and their sustained global warming potential
665 (SGWP). Ecosystem, water and vegetation represent flux and SGWP measured or calculated from the ecosystem by EC
666 tower, from open water and from vegetated area. The numbers in the square bracket represent the 95% confidence interval
667 of the average. No error bounds are reported for flux and SGWP from water as they are modelled using gas concentration
668 in the water and meteorological measurements.

		Ecosystem	Water	Vegetation
Flux (g C m^{-2})	CO_2	8 [-18.9, 34.9]	297.5	-39.5 [-70.8, -8.1]
	CH_4	3.9 [3.8, 4.1]	1.7	4.3 [4.1, 4.5]
SGWP (kg CO_2-eq m^{-2})	CO_2	0.029 [-0.069, 0.128]	1.090	-0.145 [-0.260, -0.030]
	CH_4	0.234 [0.225, 0.244]	0.104	0.256 [0.246, 0.268]

669

https://doi.org/10.5194/bg-2019-279
Preprint. Discussion started: 18 September 2019

Biogeosciences
Discussions
Open Access
EGU

670 **Figures**

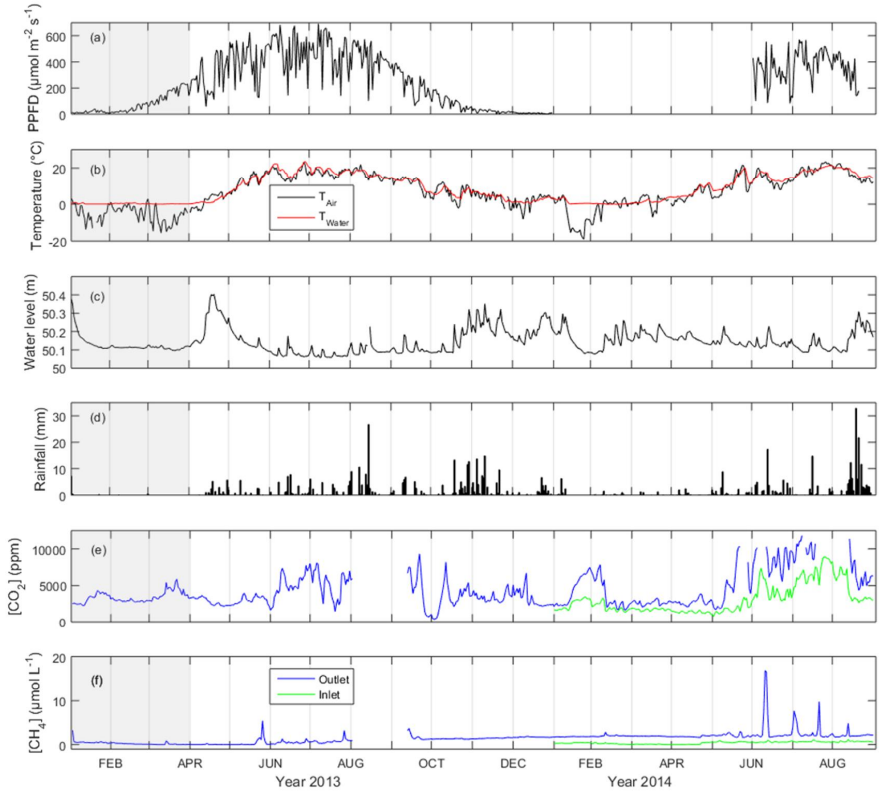

671

672 Figure 1: The daily-average of (a) photosynthetic photon flux density (PPFD), (b) air and water temperature, (c) water
673 level, (d) rainfall, (e) CO_2 concentration and (f) CH_4 concentration from inlet and outlet of Nummela wetland from
674 January 2013 to August 2014. The grey zone indicates the ice-covered period.

https://doi.org/10.5194/bg-2019-279
Preprint. Discussion started: 18 September 2019

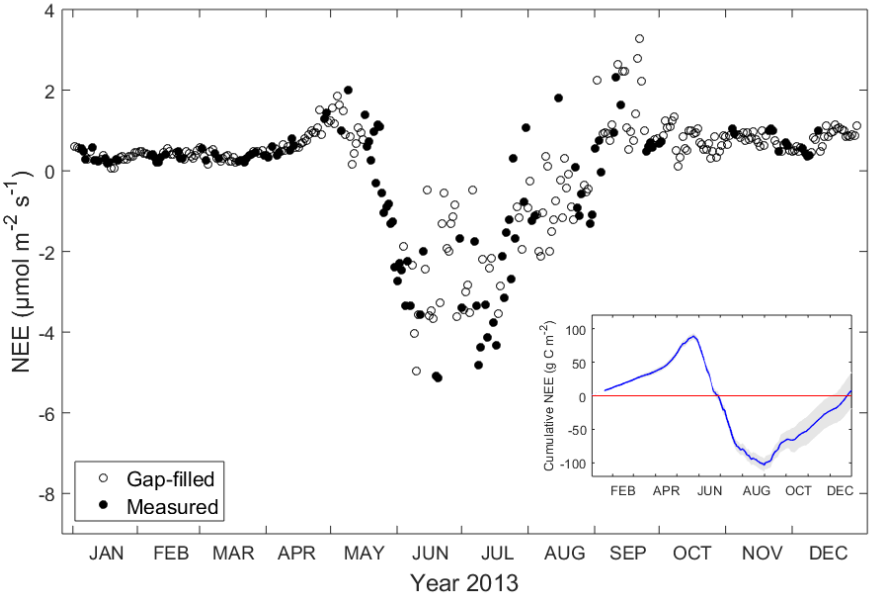

675

676 Figure 2: Daily average of net ecosystem exchange of CO_2 (NEE, µmol m^{-2} s^{-1}) in year 2013. Filled dots indicate
677 measurement (wen available half-hourly measurement data ≥ 10) and circles indicate gap-filled data (when available half-
678 hourly measurement data < 10). The insert shows cumulative NEE (g C m^{-2}) in the ecosystem and the red line indicates
679 the zero reference line. Error bounds (marked in grey) on cumulative NEE reflect the 95 % confidence interval for the
680 gap-filling procedure.

681

682

683

https://doi.org/10.5194/bg-2019-279
Preprint. Discussion started: 18 September 2019

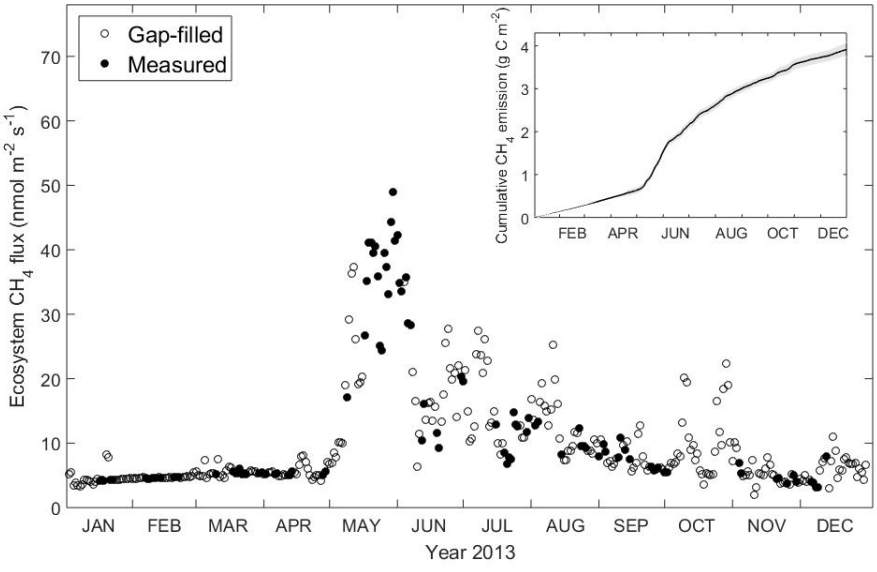

Figure 3: Daily average of ecosystem CH_4 flux measured by EC tower and cumulative CH_4 emission in year 2013. Filled dots indicate measurement (when available half-hourly measurement data ≥ 10) and circles indicate gap-filled data (when available half-hourly measurement data < 10). The insert shows cumulative CH_4 emission with the error bounds in grey reflecting the 95 % confidence interval for the gap-filling procedure.

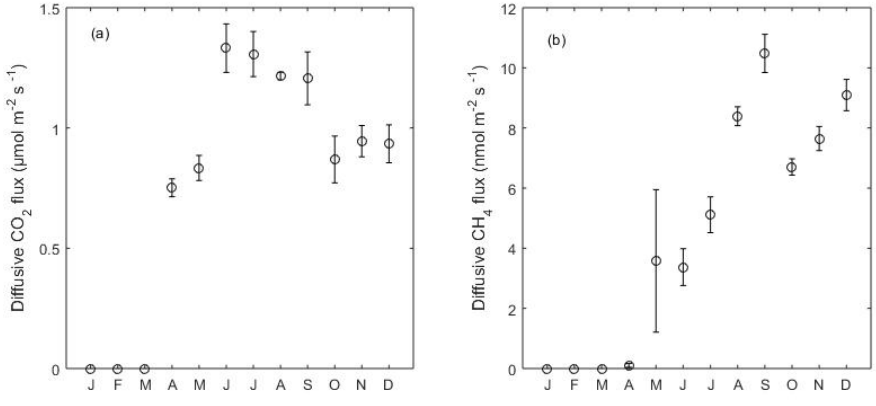

Figure 4: Monthly-average of (a) diffusive CO_2 and (b) CH_4 flux from the open-water in year 2013. Error bar indicates the standard error of the mean. From January to March there was ice-covered period.

https://doi.org/10.5194/bg-2019-279
Preprint. Discussion started: 18 September 2019

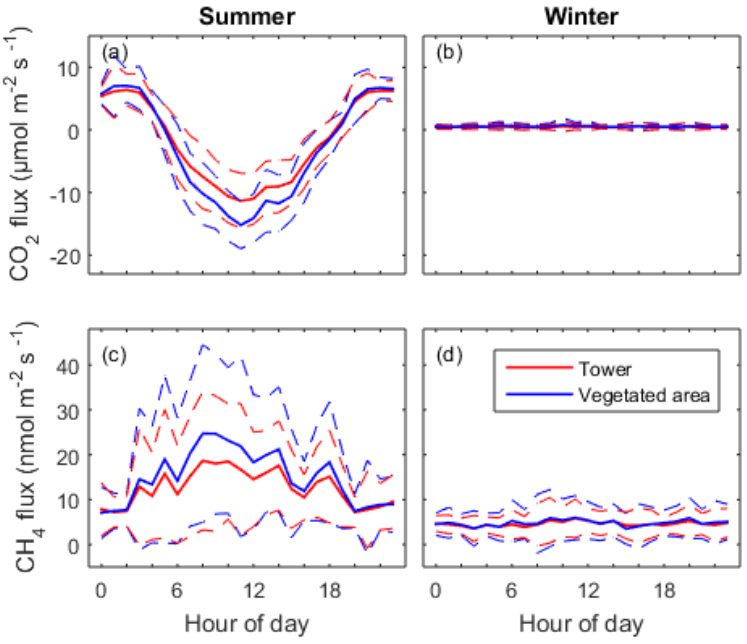

695

696 Figure 5: Mean diel pattern of the half-hourly net CO_2 and CH_4 fluxes in summer ((a) and (c)) and in winter ((b) and
697 (d)). The dashed lines represent the standard deviation. Red lines indicate measurement from EC tower and the blue
698 lines show the fluxes modelled for vegetated area.

699